Optimal Constrained Viscoelastic Tape Lengths for Maximizing Damping in Laminated Composites

P. Raju Mantena*
University of Mississippi, University, Mississippi 38677
and
Ronald F. Gibson† and Shwilong J. Hwang‡
Wayne State University, Detroit, Michigan 48202

The results of experimental investigations conducted on glass/epoxy and graphite/epoxy composite laminated beams with constrained layer surface-damping treatments are reported. A fast Fourier transform based impulse technique is used for identifying an optimal length of damping tape to be applied for maximizing the structural loss factor. This requirement stems from a need (as in helicopter rotor blade applications) for a tradeoff between the added weight of the viscoelastic layer and the resultant changes in the dynamic characteristics of the structure. The experimental data is compared with analytical results obtained by a modal strain energy/three-dimensional finite element method. This study has shown that, for a given composite structure and boundary conditions, there exists an optimum length of the constraining layer that produces maximum shear strain energy of the intermediate viscoelastic layer, thus providing maximum damping. Boundary conditions are also shown to have a strong influence on the system damping.

Introduction

SURFACE damping treatments have been in vogue for quite some time for solving a variety of resonant noise and vibration problems—especially those associated with vibration of sheet metal structures. Such treatments, which capitalize on the inherent damping of a highly dissipative material, can easily be applied as a single layer (as with auto undercoatings) to one or both sides of existing structures and provide high damping capability over a wide temperature and frequency range. In the case of the free-layer (also referred to as extensional or unconstrained) damping treatment, when the base plate bends, the amount of energy absorbed per oscillation depends on the mean longitudinal strain induced in the coating. The degree of damping is therefore limited by thickness and weight restrictions. On the other hand, for a given weight, the shear type of damping treatment, which can be obtained by the application of commercially available damping tapes to the base structure, is found to be more efficient than the unconstrained-layer damping treatment. Since shear deformation is considered to be one of the major mechanisms by which energy is dissipated in polymeric adhesives, the large shear strains produced in the intermediate adhesive layer provide considerable damping. This is the basic principle that is exploited in constrained-layer damping treatments.

For facilitating the desired performance, parameters other than temperature and frequency (namely geometry, stiffness, mass, and mode shape of the structure to which the control system is applied) will also equally affect the performance. The methods of analysis for such free-layer and constrained-layer damping systems were developed by Ross-Kerwin-Ungar (referred to as the RKU analysis) in the 1950s[1] and have been most widely used for predicting the structural response under both extensional and shear deformations. Application of this RKU method with improvements and/or modifications thereof for noise reduction in helicopter cabins and diesel engines, and for vibration control in jet engine inlet guide vanes and aircraft weapons dispensers are reported by Jones,[2,3] Rogers and Nashif,[4] Jones et al.,[5] and Nashif and Nicholas,[6] respectively. Ely and Sangha[7] and Ely[8] report of advanced designs for an A-7 center section and the F-111 outboard spoiler using constrained-layer damping treatment that extended their service life by a factor of at least 50. About one-half of that improvement was attributed to constrained layers of AF-32 adhesive, and the remainder of the improvement was due to changes in materials, shapes, forming, and fastening.

Almost all the reported applications were designed, however, to improve the dynamic response of isotropic metallic structural elements. To the authors' knowledge, there has been a very limited number of previous applications[9,10] of constrained layer damping treatments for vibration control of anisotropic composite structural elements. In the recent past, an exhaustive study of the optimization of the internal material damping of various types of advanced composites has been undertaken. These analytical and experimental investigations included aligned short fiber composites,[11,12] aligned short fiber off-axis composites,[13-15] randomly oriented short fiber composites,[16] and two- and three-dimensional modeling of laminated composites.[17-21] Parameters such as loading angle, fiber aspect ratio, fiber tip spacing, ply thickness, and damping ratio between the fiber and matrix materials were adjusted to improve the performance of composite materials in a dynamic environment.

Objective and Scope of Research

Designs generated by parametric studies of the type described earlier are, however, at best locally optimal with improvements of internal material damping being restricted by the properties of the fiber and matrix materials, along with an inherent tradeoff between damping and stiffness. Many of the composite structures used in military and space applications, however, are subjected to severe dynamic loading environments where such a tradeoff may not be desirable. With enhancement of internal material damping having already been exploited to its peak level by the methods described earlier, further vibration control by the use of surface damping treatments to reduce resonant displacements and noise

Received Nov. 20, 1989; revision received Aug. 14, 1990; accepted for publication Sept. 13, 1990.

*Assistant Professor, Department of Mechanical Engineering.
†Professor, Department of Mechanical Engineering, 2140 Engineering Building.
‡Research Associate, Department of Mechanical Engineering, 2140 Engineering Building.

level provides the scope for exploratory studies of the type reported in this paper.

As such, the objective of this research was to demonstrate the potential for improvement and optimization of damping in laminated anisotropic composite structures with constrained viscoelastic layer damping tapes. The influence of damping tape distribution and boundary conditions on damping of different modes, in unidirectional and off-axis glass/epoxy and graphite/epoxy composite beams were investigated. Experimental data generated by a fast Fourier transform based impulse technique was compared with analytical predictions obtained by a modal strain energy/three-dimensional finite element method.

Experimental Procedures

A 12 × 12 in. (304.8 × 304.8 mm), 16-ply unidirectional aligned continuous E-glass/epoxy (3M Scotchply 1003) composite plate with a thickness of 0.13 in. (3.3 mm) was fabricated as per manufacturer's specifications, using an autoclave-style process.[22] Cantilever beam specimens 5 in. long × 1 in. wide (127 × 25.4 mm) were machined from this plate. Similarly, unidirectional and 20-deg off-axis graphite/epoxy specimens having dimensions of 8 in. long × 0.75 in. wide × 0.057 in. thick (203.2 × 19.05 × 1.45 mm) were machined from a laminated plate fabricated with 12 plies of Fiberite Hy-E1034C (T300 graphite fibers/934 epoxy resin) prepreg tape. Baseline loss factor data were obtained for these bare specimens by testing them as cantilever beams for different span lengths (to get the frequency dependency) using the impulse-frequency response vibration technique.

In the impulse-frequency response technique, the specimen is excited by using an impulse hammer with a piezoelectric force transducer in its tip. The specimen response is measured by a noncontacting eddy current proximity transducer, located away from the nodal points. By curve fitting the resonant peak of the Fourier-transformed frequency response function displayed on the screen of the spectrum analyzer, the loss factor (a measure of damping) of the composite specimens is obtained with the half-power bandwidth relationship:

$$\eta = \frac{\Delta f}{f_n} \tag{1}$$

where Δf is the half-power bandwidth of resonant peak frequency response curve at resonant frequency f_n. For further details of the impulse-frequency response technique the reader is referred to Ref. 23.

Damping tape (3M type SJ-2052X) having a 0.005 in. (0.127 mm) thick ISD 112 acrylic polymer viscoelastic adhesive and a 0.01 in. (0.254 mm) thick dead soft aluminum backing as the constraining layer was then applied on one side of the glass/epoxy and graphite/epoxy specimens comprising the base structure for different ratios of tape length to cantilever beam length (T/L). Loss factor data was again obtained for different boundary conditions such as tape fixed at root (i.e., at clamped end), tape free at root, and for tape applied about 0.5 in. (12.7 mm) from the clamped end, as shown in Fig. 1. The effects of tape distribution on both sides of the base structure for conditions of $T/L < 0.5$ (i.e., toward the clamped end) were also investigated for both fixed- and free-tape boundary conditions at the root. By distributing the tape on both sides of the base structure nearer to the clamp (simulating the hub of a helicopter rotor blade), centrifugal and drag forces that would otherwise shear off the tape edgewise from the rotating blades (if it was distributed more toward the tip end) can be minimized. Both first- and second-mode loss factor data were obtained, with three specimens tested in each category. Because of space limitations only the first-mode data is presented in this paper, however.

Modal Strain Energy/Finite Element Method

The resulting experimental data was compared with the analytical predictions obtained by a modal strain energy/three-dimensional finite element method. The strain energy method has been proven to be an accurate and flexible technique for determining damping of structures. The concept of damping in terms of strain energy quantities was apparently first introduced by Ungar and Kerwin[24] who developed Eq. (2) for the loss factor of an arbitrary system of linear viscoelastic elements,

$$\eta = \frac{\sum_{i=1}^{N} \eta_i W_i}{\sum_{i=1}^{N} W_i} = \sum_{i=1}^{N} \left(\frac{\eta_i W_i}{W_t}\right) \tag{2}$$

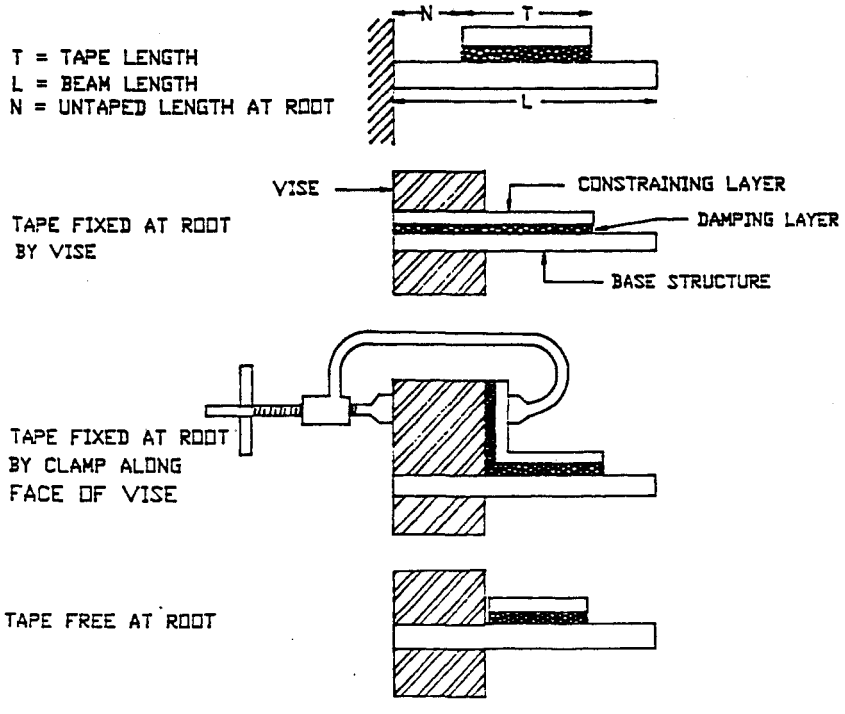

Fig. 1 Distribution and boundary conditions of the damping tape applied on one side of the composite base structure.

where η_i is the loss factor of the ith element, W_i is the strain energy stored in the ith element, W_t is the total strain energy stored in the composite, and N is the number of elements in the structure.

The assumption of linear viscoelastic behavior was valid for the present research, as experiments showed that the damping and stiffness were independent of vibratory strain levels. As such, the strain energy method was implemented in a three-dimensional finite element formulation for predicting damping of the composites treated with constrained-layer damping treatments.

The finite element method (FEM) has also been widely used in structural dynamic analysis of constrained viscoelastic laminates.[25] Some of the work has involved the prediction of damping with a three-dimensional FEM on isotropic base structures treated with continuous layers of damping tapes.[26-28] The motivation for using three-dimensional FEM in this research is that, by including the three-dimensional stress state for complex geometry (i.e., variations of cross section due to application of constrained-layer damping tape for different ratios of tape to beam length) and boundary conditions, a more realistic analysis would result. As such, the actual analysis involves the modal strain energy method as suggested by Johnson et al.[26] and Johnson and Kienholz[27] and implemented in a finite element formulation of the SAP IV (chosen for its anisotropic material capabilities and ease of modification) program[29] by Hwang and Gibson[19] and Hwang.[20] The computer program 3DFEM,[20] which incorporates the modal strain energy/finite element method, was used in this research for the analytical modeling of the anisotropic composite structures treated with damping tapes.

By this approach, an eigenvalue/eigenvector problem of a free-vibration analysis is performed using the finite element method. The structural loss factor for each mode of vibration is calculated by using the mode shape and the loss factor for each material. That is, the strain energy is calculated based on the resulting eigenvector (mode shape) without concerning the real amplitude of the mode shape. For example, the element strains are calculated by using the strain-displacement relationship, where the strain-displacement transformation matrix is evaluated by the FEM:

$$[\epsilon] = [B]\,[U] \tag{3}$$

where $[\epsilon]$ is the element strain matrix corresponding to rth mode, $[B]$ is the element strain-displacement transformation matrix, and $[U]$ is the element nodal displacement matrix in global coordinates corresponding to eigenvector for rth mode.

The corresponding element stresses are then evaluated by using the stress-strain relationship:

$$[\sigma] = [C]\,[\epsilon] \tag{4}$$

where $[\sigma]$ is the element stress matrix, and $[C]$ is the element stiffness matrix.

It may be noted that the difference between isotropic and anisotropic analysis resides in the element stiffness matrix $[C]$ in Eq. (4). Due to the anisotropic nature of the composite base structure, further decomposition of the strain energy terms into terms associated with different stress components is also required.[20] The element strain energy W_{ij} due to each of the six resulting stresses σ_{ij} (i.e., three in-plane stresses and three interlaminar stresses) is calculated by numerical integration of Eq. (5) over the element volume V:

$$W_{ij} = \frac{1}{2}\int_v \sigma_{ij}\,\epsilon_{ij}\,dv, \qquad i,j = 1,2,3 \tag{5}$$

where the repeated subscripts i and j do not imply summation.

The loss factor of the overall structure (with the applied damping treatment) is finally formulated as the weighted average of the loss factors of the constituents (i.e., base structure, damping layer, and constraining layer) along with their respective strain energies as weighting constants. Thus, the general Ungar-Kerwin Eq. (2) can be used to find the structural loss factor for a composite structure at a macromechanical level as

$$\eta_s = \frac{D_a + D_b + D_c}{W_s} \tag{6}$$

where

$$D_a = \sum_{k=1}^{l} \overset{(k)}{\eta}_{a,ij}\; W_{a,ij}^{(k)}$$

$$D_b = \sum_{k=1}^{m} \overset{(k)}{\eta}_{b,ij}\; W_{b,ij}^{(k)}$$

$$D_c = \sum_{k=1}^{m} \overset{(k)}{\eta}_{c,ij}\; W_{c,ij}^{(k)}$$

$\overset{(k)}{\eta}_{p,ij}$ = loss factor of element k in layer p due to stress component σ_{ij}

$W_{p,ij}^{(k)}$ = strain energy of element k in layer p due to stress component σ_{ij}

$p = a, b,$ or $c, \qquad i,j = 1,2,3$

The subscripts s, a, b, and c refer to the total structure, adhesive layer, base (composite) structure, and constraining layers, respectively. Also l, m, and n are the total elements in the adhesive layer, base structure, and constraining layer, respectively.

The loss factor of the constituent materials (η_a, η_b, η_c) can usually be obtained by the elastic-viscoelastic correspondence principle, manufacturers data, or experimental methods. To apply Eq. (6), the corresponding strain energy terms have to be calculated, however. As such, the computer program 3DFEM[20] was used to model the complex geometries and boundary conditions of the composite base structure treated with constrained-layer damping tapes. Analysis was performed for the tape applied on one and on both sides of the base structure, separately. To obtain more confidence in the finite element calculations of strain energy, some simple models based on a cantilever beam under free vibration were initially tested until a convergent solution of strain energy was obtained. The finite element model was started with a network of larger elements, and the element size in the laminate length direction was reduced to determine the optimum number of elements for convergence.

Based on these initial strain energy convergence studies, a 420-element model (with 6768 degrees of freedom) was chosen for the current analysis. The model used had only one element in both the width and thickness directions, however. This was decided based on an initial sample model of nine elements, with three elements in each of the length, width, and thickness directions. From the trial runs, it was observed that the resulting displacement data varied only along the length direction and remained essentially the same along the width and thickness directions. This is valid for flexural modes of vibration since no coupling stiffnesses are present (i.e., $B_{ij} = 0$). It is not true, however, for other modes (twisting) since the resulting displacement data is no longer constant along any direction. Since the strain energy was being calculated from the resulting mode shapes (i.e., displacements) and with the displacement data remaining constant in both the width and thickness directions, only one element was believed to be sufficient in each of these two directions. This also simplified the model and saved computer time.

Optimum aspect ratios (length/thickness) of the three-dimensional eight-node thick shell elements used for modeling the different layers that constitute the composite structure were also selected. Figure 2 shows a typical gridwork for a composite specimen with a damping tape-to-beam length ratio

I.D.	Element	Aspect Ratio (length/thickness)
A	Adhesive Layer	7.144:1
B	Base Structure	0.275:1
C	Constraining Layer	3.572:1

N/L = 0 T/L = 0.6
Number of Elements = 308
Number of Nodes = 904
Number of Degrees of Freedom = 2700
Total Solution Time = 334.79 sec.
(IBM 4341 Main Frame System OS/VS1)

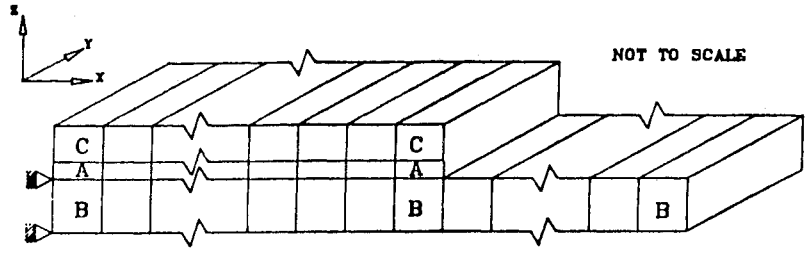

Fig. 2 Typical three-dimensional finite element model of constrained layer damping treatment on a composite base structure (with tape free at clamped end).

Table 1 Composite structure constituent material properties

	Density, ρ	Longitudinal modulus, E_1	Transverse modulus, E_2	Shear modulus, G_{12}	Poisson's ratio, ν_{12}	Fiber volume fraction, v_f	Loss factor (at 70° F) Mode 1	Loss factor (at 70° F) Mode 2
Base structure								
E-Glass epoxy [16 ply/0 deg/0.13 in. thick]	1.90 g/cm^3 (0.07 lb/in.^{3})	36 GPa (5.25 MPsi)	11 GPa (1.58 MPsi)	3 GPa (0.44 MPsi)	0.28	0.50	0.0040[a] (at 140 Hz)	0.0035[a] (at 880 Hz)
Graphite epoxy [12 ply/0 deg/0.06 in. thick]	1.58 g/cm^3 (0.06 lb/in.^{3})	127 GPa (18.55 MPsi)	10.27 GPa (1.49 MPsi)	7.31 GPa (1.49 MPsi)	0.22	0.67	0.0029 (at 55 Hz)	0.00372 (at 330 Hz)
Constraining layer								
Dead soft aluminum foil [Type 1100/0.11 in. thick]	2.76 g/cm^3 (0.1 lb/in.^{3})	69 GPa (10 MPsi)	69 GPa (10 MPsi)	26 GPa (3.79 MPsi)	0.32	—	0.033[b]	—
Damping layer								
3M SJ-2052X [ISD – 112/0.005 in. thick]	0.98 g/cm^3 (0.04 lb/in.^{3})	1.76 MPa (255 Psi)	1.76 MPa (255 Psi)	0.59 MPa (85 Psi)	0.49	—	0.87[c] (at 55 Hz)	—
	0.98 g/cm^3 (0.04 lb/in.^{3})	3.72 MPa (540 Psi)	3.72 MPa (5.40 Psi)	1.24 MPa (180 Psi)	0.49	—	—	0.90 (at 330 Hz)

[a]Measured directly. [b]Measured indirectly from taped aluminum beam. [c]From 3M data.

of 0.6 and with a free boundary condition for the tape at the clamped end. Typical solution times for such models ranged from 250 to 500 s (CPU) on an IBM 4341 mainframe system. Constituent material properties used in the analytical models are shown in Table 1. The longitudinal modulus E_1, the transverse modulus E_2, and the shear modulus G_{12} of the anisotropic base structure shown in the table are used for a complete analysis. Because of the frequency and temperature sensitivity of both the shear modulus and loss factor of the ISD 112 viscoelastic adhesive in the damping tape, appropriate data based on nomographs supplied by the manufacturer[30,31] were used to account for the differences in frequency between mode 1 and mode 2. Also, the Poisson's ratio ν for the nearly incompressible viscoelastic adhesive was taken as 0.49 (instead of 0.5), to avoid numerical difficulties.[28] With $\nu = 0.5$, the bulk modulus K approaches infinity, causing rigid-body modes in the free vibration analysis.

The loss factor of the aluminum backing (comprising the constraining layer) in the SJ-2052X damping tape was not furnished by the manufacturers. This data was required, however, as input for the three-dimensional finite element/modal strain energy method. Also, since the backing was made of Type 1100 dead soft (unalloyed) aluminum, it was believed that the material loss factor would be high enough that it could not be neglected in the analysis. As such, a combination of experimental data generation (impulse technique) and the strain energy method (three-dimensional FEM) was used along with Eq. (6) to obtain the loss factor of the constraining layer. By reverse computation, η_c was found to be 0.033. This value, which is not negligible, was used as input in all the analytical calculations/models for comparison with experimental results. For more details on the procedure adopted, the reader is referred to Ref. 10.

By looking at Eq. (6), one may immediately arrive at the "obvious" conclusion that even a highly dissipative material/element (such as the damping layer) cannot contribute significantly to the total loss factor if it does not participate considerably in the total stored strain energy. This larger contribution to the strain energy is facilitated by working the viscoelastic adhesive layer in shear (affected by the constraining layer on top) instead of pure extension.

Results and Discussion

As can be observed in Fig. 3, for the first mode of vibration, an optimized length of the viscoelastic material at which the system damping (glass/epoxy base structure with tape) is maximum is clearly evident for both the boundary conditions of tape fixed and tape free at root (i.e., at the clamped end with $N/L = 0$). Of particular interest is that for an optimum tape-to-beam length ratio of 0.6, the ratio of "taped-to-untaped" damping is significantly higher for the case where the tape is fixed at the root (by about 2.5 times) than for the case where the tape is free at root. The existence of an optimized length of viscoelastic material for which the structural damping is maximum was also observed by Plunkett and Lee.[32] Their investigations were limited, however, to applications for metallic

materials and the effects of tape boundary conditions were not taken into account.

For the condition where the tape was applied at a distance of 0.5 in. (12.7 mm) from the clamped end ($N/L = 0.1$), Fig. 4 shows that the damping effectiveness, although improved, is not as significant as for the previous two cases. This is not surprising since, in the first mode of flexural vibration, the most highly stressed region is at the clamped end. With no tape in this region to provide the additional damping mechanism (by shear deformation of the viscoelastic adhesive), the overall improvement is minimal. The experimental results (with scatter) obtained with the impulse hammer technique show fair agreement with finite element analytical predictions. Better agreement is expected if the data on complex shear modulus of the damping layer are available in the form of accurate regression equations. The results shown here are based on estimates from nomographs.

Figure 5 once again shows a comparable improvement in total damping for both fixed and free boundary conditions of the damping tape as applied to the unidirectional graphite/epoxy base structure. The damping ratio is not so significant, however, for the off-axis graphite/epoxy specimens (Fig. 6). This is because, with the 20-deg off-axis case, the base structure itself exhibited a high intrinsic loss factor (about 0.0134 for mode 1).

The critical observation that by fixing the constrained-layer tape at the clamped end, significantly higher overall damping could be obtained was further investigated. This has important ramifications by way of added weight tradeoffs when such surface damping treatments are planned, for example, in helicopter rotor blade applications. As such, the amount of damping tape (and its added weight) required to produce a given improvement in damping can be significantly reduced by clamping the tape at the fixed end of the beam. To simulate

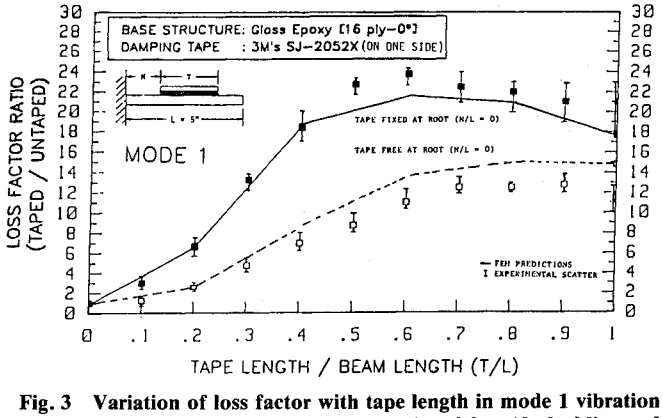

Fig. 3 Variation of loss factor with tape length in mode 1 vibration for fixed (continuous line and dark squares) and free (dashed line and plain squares) boundary conditions at root, with a unidirectional glass/epoxy composite base structure.

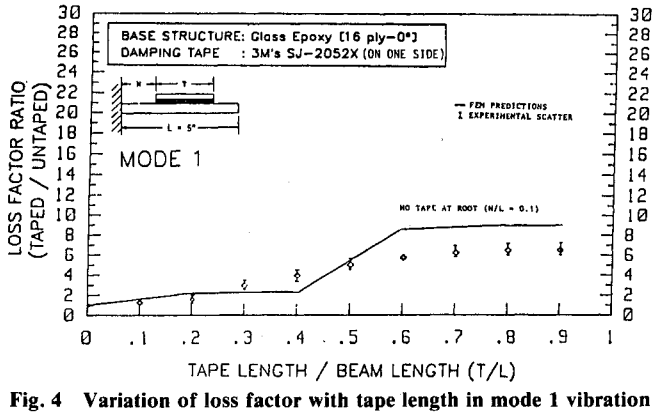

Fig. 4 Variation of loss factor with tape length in mode 1 vibration for no tape at root boundary condition, with a unidirectional glass/epoxy composite base structure.

better the finite element model of the tape being fixed at root, some experiments were repeated by fixing the tape at the root with a clamp along the face of the vise instead of having the tape inside the vise (Fig. 1). Apparent increases in damping are also possible due to the viscoelastic adhesive being located inside the vise (clamping losses). As shown in Table 2, the damping effectiveness is once again comparably higher than for the free-at-root boundary condition. The marginal variations in the loss factor data presented here with the data in Fig. 3 are attributed to a different batch of damping tape that was used for these tests.

The increased through-the-thickness shear strain energy in the adhesive as a result of fixing the tape at the root is responsible for the increase in the system damping. This is easily verified by observing the shear strain energy ratio for the fixed vs free boundary conditions at root, as shown in Fig. 7 for the first mode of flexural vibration for different lengths of tape applied to a glass/epoxy base structure. This ratio of shear strain energy was obtained from the three-dimensional finite element method by dividing the through-the-thickness shear strain energy component [refer to Eq. (5)] of the adhesive for the fixed-at-root boundary condition by the corresponding component of shear strain energy for the free-at-root boundary condition. Figure 7 shows that by fixing the tape at the root, the intermediate adhesive layer generates a larger shear strain energy as compared with not fixing the tape at the root. The likely explanation is that the aluminum constraining layer on the top of the damping tape is stiffened by fixing it at the base and as such is causing larger average shear deformations in the viscoelastic adhesive layer. This larger average shear deformation in the adhesive gradually decreases for tape lengths over 0.6 times the beam length for the first

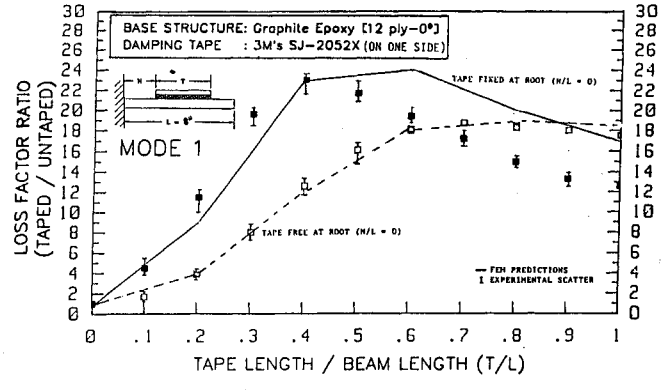

Fig. 5 Variation of loss factor with tape length in mode 1 vibration for fixed (continuous line and dark squares) and free (dashed line and plain squares) boundary conditions at root, with a unidirectional graphite/epoxy composite base structure.

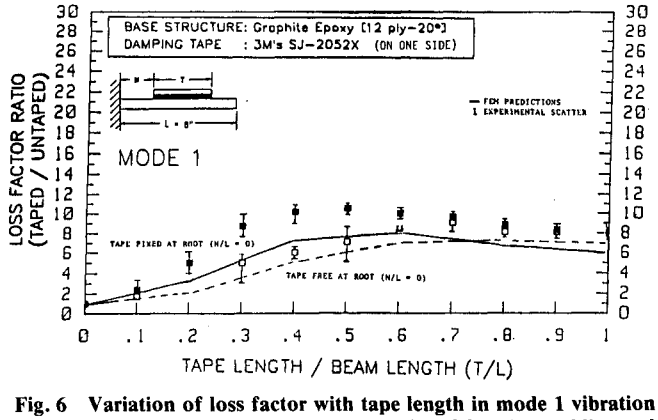

Fig. 6 Variation of loss factor with tape length in mode 1 vibration for fixed (continuous line and dark squares) and free (dashed line and plain squares) boundary conditions at root, with a 20-deg off-axis graphite/epoxy composite base structure.

Table 2 Typical experimental data on the influence of tape boundary conditions (at the clamped end of the beam) on system damping

	Loss factor (untaped) Glass/epoxy specimens[a]	Damping with different tape boundary conditions: Free at root		Fixed (along face of vise)		Fixed (inside vise)	
		Loss factor (taped)	Loss factor ratio	Loss factor (taped)	Loss factor ratio	Loss factor (taped)	Loss factor ratio
Mode 1	0.0040	0.049	12.2	0.070	17.5	0.080	20.3
Mode 2	0.0035	0.029	8.3	0.047	13.3	0.043	12.3

[a]Note: average of three specimens with $N/L = 0.0$, $T/L = 0.5$.

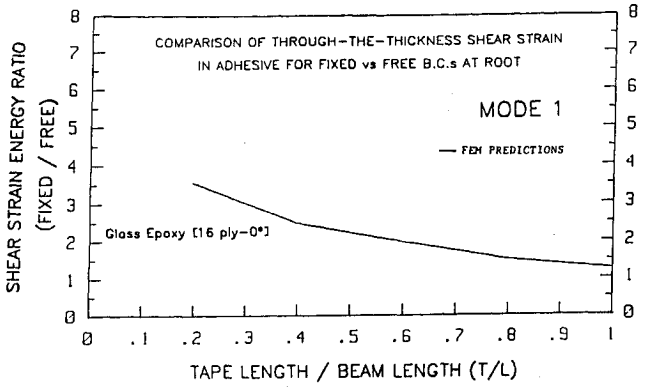

Fig. 7 Analytical predictions of through-the-thickness shear strain in adhesive for fixed vs free boundary conditions at root, in mode 1 vibration.

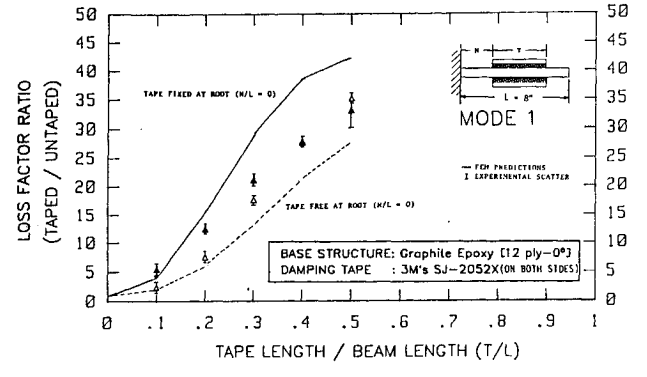

Fig. 8 Variation of loss factor with tape length in mode 1 vibration for fixed (continuous line and dark squares) and free (dashed line and plain squares) boundary conditions at root, with a tape applied on both sides of unidirectional graphite/epoxy composite base structure.

mode of flexural vibration. This further reaffirms the fact that there is an optimum tape length at which maximum structural damping can be obtained.

Similar conclusions on the effects of boundary conditions were reported by Mead and Markus[33] who developed a closed-form analytical solution for sandwich beams with fixed, free, and simply supported boundary conditions. Their results suggest that the effect of boundary conditions depends on the frequency range, however, and that the maximum system loss factor is not very sensitive to boundary conditions. A direct comparison of the present results with those of Mead and Markus is not possible because the present work is concerned with discontinuous damping layers whose complex shear modulus varies with frequency, whereas Mead and Markus analyzed continuous damping layers whose complex shear modulus was assumed to be independent of frequency.

Table 3 shows the percentage contribution of the constituent materials (base structure, adhesive layer, and constraining layer) to system damping for the first mode of flexural vibration. These results were summarized from the three-dimensional finite element/strain energy analytical models for different tape-to-beam length ratios and with tape free

Table 3 Contribution of constituent materials to system damping in the first mode of vibration (analytical data with tape free at root)

T/L[a]	I.D. of base structure[b]	Percentage of total damping[c] F_a	F_b	F_c
0.2	1	64.8	34.4	0.8
	2	69.6	25.6	4.8
	3	50.8	45.6	3.6
0.4	1	89.0	10.2	0.8
	2	89.3	7.7	3.0
	3	79.6	17.6	2.8
0.6	1	92.7	6.2	1.1
	2	91.9	5.0	3.1
	3	85.3	11.8	2.9
0.8	1	93.0	5.5	1.5
	2	91.6	4.6	3.8
	3	85.4	11.2	3.4
1.0	1	92.5	5.5	2.0
	2	91.0	4.7	4.3
	3	84.8	11.4	3.8

[a]T/L = tape length to beam length ratio.
[b]I.D. of base structure: 1) E-glass/epoxy (0 deg) at 150 Hz, 2) graphite/epoxy (0 deg) at 55 Hz, 3) graphite/epoxy (20 deg) at 35 Hz.
[c]F_a = percentage of damping in adhesive layer, F_b = percentage of damping in base structure, F_c = percentage of damping in constraining layer.

at root boundary condition. Such an analysis capability is one of the inherent advantages of the finite element/strain energy approach. It is obvious from these results that, as expected, the viscoelastic adhesive layer has the maximum contribution to the overall system damping, increasing with increasing tape application. It is also apparent that the contribution of the anisotropic base structures to system damping is high, with the off-axis graphite/epoxy specimens leading the other two unidirectional glass/epoxy and graphite/epoxy base structure material configurations. The contribution of the aluminum constraining layer to overall system damping is very low, however, as it should be.

As mentioned earlier, one of the problems of locating the add-on damping tape at the free end of a rotating cantilever structure (such as a helicopter rotor blade) is that the high centrifugal and edgewise drag forces generated in this region are likely to shear off the tape from the base to which it is attached. Application of the damping tape on both sides of a rotating base structure has practical advantages also in that by symmetrically wrapping the add-on material, exposure of the tape's layered edges to opposing drag forces can be eliminated. Superposition and symmetry should also lead to increases in damping by a factor of two. As such, investigations were carried out for optimizing damping performance by distributing the damping tape on both sides toward the base structure (i.e., for tape-to-beam length ratios less than 0.5). Figure 8 shows the results of the experimental investigations using the impulse hammer technique and the three-dimensional finite element/strain energy method for both the fixed and free at root boundary conditions of the damping tape applied to unidirectional graphite/epoxy composite specimens. It may be noted that the theoretical predictions of loss factor is higher than experiment for tape-to-beam length ratios beyond 0.2. This is also consistent with the observations of

Fig. 5 (with tape on one side) for tape-to-beam length ratios beyond 0.4. Both are equivalent, since the same amount of damping tape applied on one side (Fig. 5) was redistributed on both sides for the other case (Fig. 8). The sharp "knee" observed at 0.1 of the tape-to-beam length (T/L) ratio in Fig. 8 is also consistent with the sharp "knee" at $T/L = 0.2$ in Fig. 5. It is worth mentioning that although the horizontal axis for both Figs. 5 and 8 are the same, the vertical scale of Fig. 8 is almost double that of Fig. 5, however. By careful comparison with Fig. 5 (for tape on one side), it is clear that comparable levels of damping can be obtained by distributing the same amount of tape on both sides instead of all of it on one side. For the particular case of tape on one side, for a T/L of 0.6 (Fig. 5, experimental data for tape fixed at root, i.e., dark squares) the loss factor ratio is around 24 vs 22 for the tape applied on both sides and a T/L ratio of 0.3 (Fig. 8, dark triangles). This is essentially for an equivalent quantity of tape. But for the tape distributed entirely on one side, the loss factor ratio is only 12 (Fig. 5, $T/L = 1.0$) as compared with around 33 obtained by distributing the same quantity of tape on both sides up to half the length of the beam (Fig. 8, $T/L = 0.5$)! As before, the system damping is higher for the tape-fixed-at-the-root condition than for the tape-free-at-the-root condition.

Conclusions

This research has demonstrated the feasibility of using viscoelastic damping materials in the form of constrained-layer damping tapes for vibration control of anisotropic composite structural elements so as to reduce resonant displacements and noise levels in severe dynamic environments. Measurement and predictions show that, for a given composite cantilever beam vibrating in a given mode, there is an optimum damping tape distribution for maximum damping. Significant improvements in damping were predicted and measured when the constraining layer was clamped at the fixed end of the beam. The amount of damping tape (and its added weight) required to produce a given improvement in damping can be significantly reduced by clamping the tape at the fixed end of the beam. Comparable improvements in damping can be obtained by applying the same amount of tape equally distributed on both sides of the structure in the region of maximum bending stress (i.e., at the clamped end for a cantilever beam). Once again, by clamping the tape at the fixed end (on both sides), better performance can be achieved without sacrificing weight. The viscoelastic layer damping treatments were less effective for off-axis composite structures because of the relatively high inherent damping in the composite itself in the off-axis configuration. The total system damping is comparable, however. The three-dimensional finite element implementation of the modal strain energy method proved to be a powerful analytical tool for predicting damping of such complex systems. Finally, the impulse-frequency response technique proved to be a fast and accurate method for measuring damping in such anisotropic composite structures treated with constrained-layer damping tapes.

Acknowledgments

The support of the Army Research Office Grant No. DAAL03-88-K-0013 (Program Manager—Gary Anderson) through a subcontract from the University of Florida is gratefully acknowledged. The authors are also indebted to Dwayne Nelson of the 3M Company, St. Paul, Minnesota, for the time spent in fruitful discussions and for supplying the damping tapes. This research was performed when the authors were in the Mechanical Engineering Department, University of Idaho, Moscow, Idaho.

References

[1]Ross, D., Ungar, E. E., and Kerwin, E. M., Jr., "Damping of Plate Flexural Vibrations by Means of Viscoelastic Laminate," *Structural Damping,* American Society of Mechanical Engineers, New York, 1959, pp. 49–88.

[2]Jones, D. I. G., "Effect of Free Layer Damping on Response of Stiffened Plate Structure," *Shock and Vibration Bulletin,* Vol. 42, Part II, Dec. 1970, pp. 105–120.

[3]Jones, D. I. G., "Design of Constrained Layer Treatments for Broad Temperature Damping," *Shock and Vibration Bulletin,* Vol. 44, Part V, 1974.

[4]Rogers, L. C., and Nashif, A. D., "Computerized Processing and Empirical Representation of Viscoelastic Material Property Data and Preliminary Constrained Layer Damping Treatment Design," *Shock and Vibration Bulletin,* Vol. 48, Part II, 1978, p. 23.

[5]Jones, D. I. G., Nashif, A. D., and Parin, M. L., "Parametric Study of Multiple-Layer Damping Treatments on Beams," *Journal of Sound and Vibration,* Vol. 29, No. 4, 1973, pp. 423–434.

[6]Nashif, A. D., and Nicholas, T., "Vibration Control by a Multiple-Layered Damping Treatment," *Shock and Vibration Bulletin,* Vol. 41, Part II, 1970, pp. 121–131.

[7]Ely, R. A., and Sangha, K. B., "Prediction and Measurement of Damping of Vibrations of Structures by Adhesives," *Proceedings of Advancing Technology in Materials and Processes, 30th National SAMPE Symposium and Exhibition,* Vol. 30, Society for Advancement of Material and Process Engineering, Covina, CA, March 1985.

[8]Ely, R. A., "Laminated Damped Aircraft Structures," ASME Winter Annual Winter Meeting, New Orleans, LA, Dec. 1984.

[9]Sun, C. T., Sankar, B. V., and Rao, V. S., "Damping and Vibration Control of Unidirectional Composite Beams Using Add-On Viscoelastic Materlals," 59th Shock and Vibration Symposium, Albuquerque, NM, Oct. 1988.

[10]Mantena, P. R., "Vibration Control of Composite Structural Elements with Constrained Layer Damping Treatments," Ph.D. Dissertation, Mechanical Engineering Dept., Univ. of Idaho, Moscow, ID, Aug. 1989.

[11]Gibson, R. F., Chaturvedi, S. K., and Sun, C. T., "Complex Moduli of Aligned Discontinuous Fiber-Reinforced Polymer Composites," *Journal of Materials Science,* Vol. 17, 1982, pp. 3499–3509.

[12]Gibson, R. F., Sun, C. T., and Chaturvedi, S. K., "Damping and Stiffness of Aligned Discontinuous Fiber Reinforced Polymer Composites," *Proceedings of the 23rd AIAA/ASME/ASCE/AHS Structures, Structural Dynamics and Materials Conference,* AIAA, Washington, DC, May 1982, pp. 247–255.

[13]Sun, C. T., Chaturvedi, S. K., and Gibson, R. F., "Internal Damping of Short Fiber Polymer Matrix Composites," *Computers and Structures,* Vol. 20, No. 1-3, 1985, pp. 391–400.

[14]Sun, C. T., Gibson, R. F., and Chaturvedi, S. K., "Internal Damping of Polymer Matrix Composites Under Off-Axis Loading," *Journal of Materials Science,* Vol. 20, 1985, pp. 2575–2585.

[15]Suarez, S. A., Gibson, R. F., Sun, C. T., and Chaturvedi, S. K., "The Influence of Fiber Length and Fiber Orientation on Damping and Stiffness of Polymer Composite Materials," *Experimental Mechanics,* Vol. 26, No. 2, June 1986, pp. 175-184.

[16]Sun, C. T., Wu, J. K., and Gibson, R. F., "Prediction of Material Damping in Randomly Oriented Short Fiber Polymer Matrix Composites," *Journal of Reinforced Plastics and Composites,* Vol. 4, July 1985, pp. 262–272.

[17]Sun, C. T., Wu, J. K., and Gibson, R. F., "Prediction of Material Damping of Laminated Polymer Matrix Composites," *Proceedings of Vibration Damping Workshop II,* Air Force Wright Aeronautical Labs., Paper No. FE, March 1986.

[18]Wu, J. K., "Optimization Of Material Damping and Stiffness of Laminated Fiber-reinforced Composite Structural Elements," Ph.D. Dissertation, Dept. of Engineering Sciences, Univ. of Florida, Gainsville, FL, Dec. 1985.

[19]Hwang, S. J., and Gibson, R. F., "Micromechanical Modeling of Damping in Discontinuous Fiber Composites Using a Strain Energy/Finite Element Approach," *Journal of Engineering Materials and Technology,* Vol. 109, No. 1, 1987, pp. 47–52.

[20]Hwang, S. J., "Characterization of the Effects of Three Dimensional States of Stress on Damping of Laminated Composites," Ph.D. Dissertation, Mechanical Engineering Dept., Univ. of Idaho, Moscow, ID, May 1988.

[21]Hwang, S. J., and Gibson, R. F., "The Effects of Three Dimensional States of Stress on Damping of Laminated Composites," *Composites Science and Technology,* Vol. 41, No. 4, 1991, pp. 379–393.

[22]Gibson, R. F., Deobald, L. R., and Suarez, S. A., "Laboratory Production of Discontinuous Aligned Composite Plates Using the Autoclave-Style Press Cure," *Journal of Composites Technology Research,* Vol. 7, No. 2, 1985, pp. 49–54.

[23]Suarez, S. A., and Gibson, R. F., "Improved Impulse-Frequency Response Technique for Measurement of Dynamic Mechanical Properties of Composite Materials," *Journal of Testing and Evaluation,* Vol. 15, No. 2, 1987, pp. 114–121.

[24]Ungar, E. E., and Kerwin, E. M., Jr., "Loss Factors of Viscoelastic Systems in Terms of Strain Energy Concepts," *Journal of Acoustical Society of America,* Vol. 34, No. 2, 1962, pp. 954–958.

[25]Bogner, F. K., and Soni, M. L., "Finite Element Vibration Analysis of Damped Structures," AIAA Paper 81-0489, April 1981.

[26]Johnson, C. D., Keinholz, D. A., and Rogers, L. C., "Finite Element Prediction of Damping in Structures with Constrained Viscoelastic Layers," *Proceedings of the 51st Shock and Vibration Symposium,* San Diego, CA, Oct. 1980.

[27]Johnson, C. D., and Kienholz, D. A., "Finite Element Prediction of Damping in Structures With Constrained Viscoelastic Layers," *AIAA Journal,* Vol. 20, No. 9, 1982, pp. 17–24.

[28]Lu, Y. P., and Everstine, G. C., "More on Finite Element Modeling of Damped Composite Systems," *Journal of Sound and Vibration,* Vol. 69, No. 2, 1980, pp. 199–205.

[29]Bathe, K. J., Wilson, E. L., and Peterson, F. E., *SAP IV, A Structural Analysis Program for Static and Dynamic Response of Linear Systems,* College of Engineering, Univ. of California, Berkeley, CA, April 1974.

[30]Product Information, "Scotchdamp" Vibration Damping Tapes SJ-2052X Nomograph, Structural Products Department, 3M Center, St. Paul, MN.

[31]Nashif, A. D., Jones, D. I. G., and Henderson, J. P., *Vibration Damping,* Wiley Interscience, New York, 1985.

[32]Plunkett, R., and Lee, C. T., "Length Optimization for Constrained Viscoelastic Layer Damping," *Journal of Acoustical Society of America,* Vol. 48, 1970, pp. 150–161.

[33]Mead, D. J., and Markus, S., "Loss Factors and Resonant Frequencies of Encastré Damped Sandwich Beams," *Journal of Sound and Vibration,* Vol. 12, No. 1, 1970, pp. 99–112.